Journal of Applied Sciences 8 (19): 3316-3327, 2008
ISSN 1812-5654

Finite Element Based Fatigue Life Prediction of Cylinder Head for Two-Stroke Linear Engine Using Stress-Life Approach

[1]M.M. Rahman, [2]A.K. Ariffin, [2]S. Abdullah, [1]M.M. Noor, [1]R.A. Bakar and [3]M.A. Maleque
[1]Automotive Excellence Center, Faculty of Mechanical Engineering,
Universiti Malaysia Pahang, Locked Bag 12, 25000 Kuantan, Pahang, Malaysia
[2]Department of Mechanical and Materials Engineering, Faculty of Engineering,
Universiti Kebangsaan Malaysia, 43600 UKM, Bangi, Selangor, Malaysia
[3]Faculty of Engineering and Technology, Multi Media Universiti, Jalan Ayer Keroh Lama,
75450 Bukit Beruang, Melaka, Malaysia

Abstract: This study describes the finite element based fatigue life prediction of cylinder head for a two-stroke free piston linear engine subjected to variable amplitude loading, applicable to electric power generation. A set of aluminum alloys, cast iron and forged steel for cylinder head are considered in this study. The finite element modeling and analysis were performed utilizing the finite element analysis codes. The fatigue life analysis was carried out using finite element based fatigue analysis commercial codes. Fatigue stress-life approach was used when the piston is subjected to variable amplitude at different loading conditions. The effects of mean stress and sensitivity analysis on fatigue life are discussed. From the results, it was shown that the Goodman mean stress correction method is predicted more conservative (minimum life) results. It was found to differ significantly the compressive and tensile mean stresses. The compressive mean stress are beneficial however tensile mean stress detrimental to the fatigue life. The effect of materials and components S-N was also investigated and not found to give any large advantages, however the effect of certainty of survival was found to give noticeable advantages and it concluded that the 99.9% are fond to be design criteria. The proposed technique is capable of determining premature products failure phenomena.

Key words: Cylinder head, aluminum alloy, finite element analysis, stress-life, variable amplitude loading

INTRODUCTION

The free piston linear generator engine is the most recent application of the linear engine concept (Arshad *et al*., 2004; Mikalsen and Roskilly, 2008a). Linear piston motion is not restricted by the motion of a rotating crankshaft for conventional engines, however, that the piston is free to move between its end combustion chamber, only influenced by the gas and load forces acting upon it. This gives the linear engine some diverse characteristics most importantly variable stroke length and high control requirements. A more comprehensive background study on the history and potential advantages of the linear engine was demonstrated by Mikalsen and Roskilly (2007). A two-stroke free piston Linear Generator (LG) engine consists of a combustion engine and a linear electrical generator as a single unit without a crankshaft. Potential advantages of the linear engine concept including vibration free operation, lower production and maintenance costs and reduced frictional losses due to the mechanical simplicity, reduced heat transfer losses and NO_x emission due to the faster power stroke expansion, higher part load efficiency and multi-fuel possibilities due to the combustion optimization flexibility (Mikalsen and Roskilly, 2008b). The free piston linear engine consists of a double-ended piston, double-ended cylinder and a linear alternator. The piston is enclosed inside the double-ended cylinder where it moves freely along the cylinder's axis. The free piston engine is unique in that there is no crankshaft or any of the mechanical linkages typically found in a reciprocating internal combustion (IC) engine. The compression ratio in this engine is varying and potentially much greater than in the conventional configurations. Bulky designs are not necessary criteria to achieve substantial compression ratios in the free piston configuration (Achten, 1994; Somhorst and Achten, 1996). The schematic diagram of the two-stroke free piston linear generator engine is shown in Fig. 1. The main parts of this engine are a cylinder head, cylinder block, linear electric machine. The engine has only one moving part rigidly connecting the two pistons and the translator of the linear generator. The piston moves freely between its end combustion chamber, its motion being determined by instantaneous balance of cylinder gas forces, electric machine force and frictional forces. The cylinder head was considered as a comment

Corresponding Author: M.M. Rahman, Faculty of Mechanical Engineering, Universiti Malaysia Pahang, Locked Bag 12, 25000 Kuantan, Pahang, Malaysia Tel: +6-09-5492207 Fax: +6-09-5492244

to be study in terms of fatigue. Cylinder head of two-stroke free piston engine structures are very commonly subjected to fatigue loading. Fatigue has long been important issues in the design of free piston engine structures (Rahman *et al*., 2006, 2007). Fatigue calculations derived from the Finite Element Analysis (FEA) provide the foundation for predicting product performance throughout the entire design to manufacturing process and into the hands of customers. Better, stronger, lighter, safer and less costly; in less time have been got through simulation. Fatigue analysis can be used to determine how long a component can survive in a given service environment. For the vehicle body structure the fatigue assessment has traditionally been performed at the later part of the product development stage when prototypes are available and heavily relied upon the result of the ground fatigue tests. This process is very time consuming and often results in over-design with weight penalties, which is the major obstacle to achieve fuel economy. The fatigue design of cylinder head of two-stroke free piston is known to be a difficult and challenging task. A computational modeling of fatigue life assessment for cylinder head of two-stroke free piston engine is presented in this study. The objectives of this study is to predict the fatigue life for a cylinder head using stress-life approach, to investigate the effect of mean stress on fatigue life, the effect of material and component S-N approach on fatigue life, to effect of certainty of survival and also the fatigue behavior of aluminum alloy material using stress-life approach.

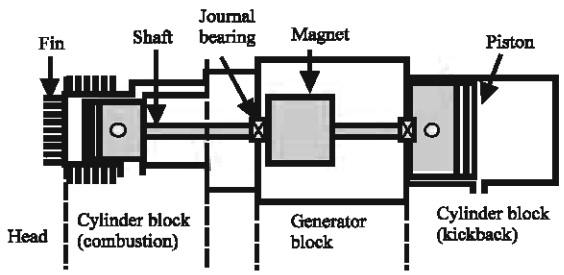

Fig. 1: A two-stroke free piston linear generator engine

FINITE ELEMENT BASED FATIGUE ANALYSIS

The fatigue analysis is used to compute the fatigue life at one location in a structure. An integrated Finite Element (FE) based fatigue analysis is considered a complete analysis of an entire component. Fatigue life can be estimated for every element in the finite element model and contour plots of life. Geometry information is provided by FE results for each load case applied independently, i.e., FE results define how an applied load is transformed into a stress or strain at a particular location in the component. Appropriate material data are also provided for the desired fatigue analysis method. The three input information boxes are descriptions of the material properties, loading history and local geometry.

All of these inputs are as followings:

- Material information-cyclic or repeated material data based on constant amplitude testing
- Load histories information-measured or simulated load histories applied to a component. The term loads is used to represent forces, displacements, accelerations, etc.
- Geometry information-relates the applied load histories to the local stresses and strains at the location of interest. The geometry information is usually derived from Finite Element (FE) results

The schematic diagram of the integrated finite element based fatigue life prediction analysis is shown in Fig. 2.

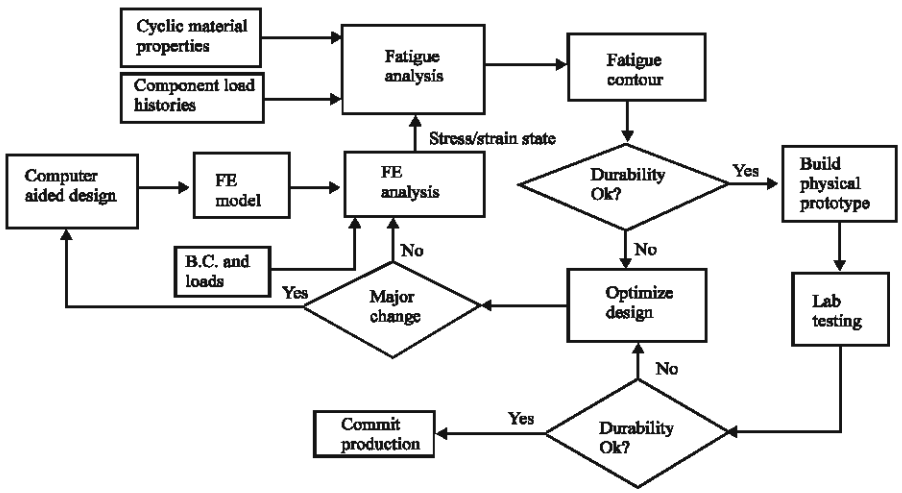

Fig. 2: Integrated finite element based fatigue life prediction analysis (Rahman *et al*., 2007)

FATIGUE ANALYSIS TECHNIQUE

Fatigue analyses can be carrying out one of three basic methodologies, i.e., the stress-life, strain-life and crack growth approaches. The stress-life approach was first applied over a hundred years ago and considers nominal elastic stresses and how they are related to life. The strain-life approach considers elastic-plastic local stresses and strains. It represents more fundamental approach and is used to determine the number of cycles required to initiate a small engineering cracks. Crack growth or Linear Elastic Fracture Mechanics (LEFM) approach is used to predict how quickly pre-existing cracks grow and to estimate how many loading cycles are required to grow these to a critical size when catastrophic failure would occur. First method is used in this paper and briefly discussed in the following sections. The Basquin showed that alternating stress versus number of cycles to failure (S-N) in the finite life region could be represented as a log-log linear relationship (Lee *et al*., 2005). The S-N approach uses to estimate the fatigue life for combined loading by determining an equivalent axial stress (Zoroufi and Fatemi, 2004) using one of the common failure criteria such as Tresca, von Mises, or maximum principal stress. The S-N Equation is mathematically given by:

$$S_e = \sigma'_f (2N_f)^b \quad (1)$$

where, S_e, σ'_f, $2N_f$ and b are the stress amplitude, the fatigue strength coefficient, the reversals to failure and the fatigue strength exponent respectively.

As shown schematically in Fig. 3, there are two inclined linear segments and one horizontal segment in atypical log-log S-N curve. The two inclined linear segments represent the Low-cycle Fatigue (LCF) and High-cycle Fatigue (HCF) regions and the horizontal asymptote represents the fatigue limit. The boundary between low and high-cycle fatigue cannot be defined by a specific number of cycles. The fatigue strength values at 1, 10^3 and 10^6 cycles define an S-N curve. These fatigue strength values referred to as S'_f, S_{1000} and S_e, respectively. Equation 2 represents the typical S-N curve. The slope of the S-N curve in the high-cycle fatigue region is denoted as b.

$$S^b N = K \quad (2)$$

where, b and K are the material parameters and N is the number of cycles to failure at a given stress amplitude, S. For low amplitudes, some materials exhibit a lower limit S_e (fatigue limit), below which fracture does not occur, i.e., N tends to infinity; statistical analysis is used in constant amplitude tests in order to estimate b and K, as well as the fatigue limit.

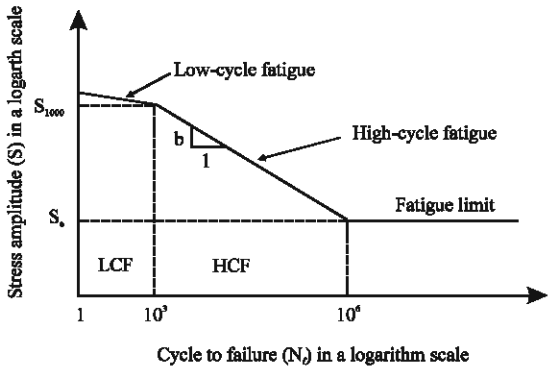

Fig. 3: A typical S-N curve

The fatigue damage of a component correlates strongly with the applied stress amplitude or applied stress range and is also influenced by the mean stress. In the high-cycle fatigue region, normal mean stresses have a significant effect on fatigue behaviour of components. Normal mean stresses are responsible for the opening and closing state of microcracks. Due to the opening of microcracks that accelerates the rate of crack propagation and the closing of microcracks retards the growth of cracks, tensile normal means stresses are detrimental and compressive normal mean stresses are beneficial in terms of fatigue strength (Lee and Taylor, 2005). The shear mean stress does not influence the opening and closing state of microcracks and not surprisingly, has little effect on crack propagation. There is very little or no effect mean stress on fatigue strength in the low-cycle fatigue region in which the large amounts of plastic deformation erases any beneficial or detrimental effect of a mean stress. Early empirical models by Gerber, Goodman were proposed to compensate for the tensile normal mean stress effects on the high-cycle fatigue strength (Lee *et al*., 2005). The modified Goodman and Gerber equations are given by Eq. 3 and 4, respectively.

$$\frac{\sigma_a}{S_e} + \frac{\sigma_m}{S_u} = 1 \quad (3)$$

$$\frac{\sigma_a}{S_e} + \left(\frac{\sigma_m}{S_u}\right)^2 = 1 \quad (4)$$

where, σ_a, S_e, σ_m and S_u are the alternating stress in the presence of mean stress, alternating stress for equivalent completely reversed loading, the mean stress and the ultimate tensile strength, respectively.

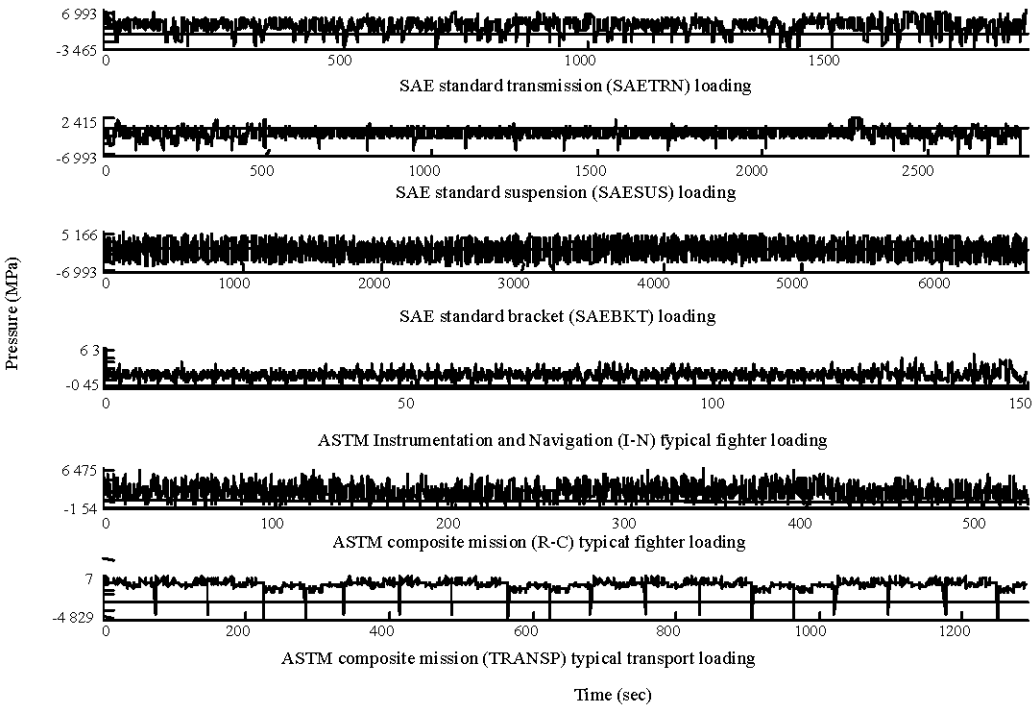

Fig. 4: The variable amplitude load-time histories

LOADING INFORMATION

Loading is another major input to the finite element based fatigue analysis. The realistic loading time histories are often difficult to obtain. A measurement of these is required during typical and extreme operating conditions. Several types of the variable amplitude loading histories were selected from the SAE and ASTM profiles for the FE based fatigue analysis. It is important to emphasize that these sequences are not intended to represent standard loading spectra in the same way that Carlos or Falstaf (Fatigure, 2005) was performed. However, they have done contain many features which are typical of the automotive industries applications and therefore, are useful in the evaluation of the life estimation methods. The component was loaded with three random time histories, corresponding to typical histories for the transmission, suspension and bracket components at different load levels. The first load history has a predominantly tensile (positive) mean which reflects sudden changes in mean, which is referred to as the transmission history. The second load history has a predominantly compressive (negative) mean, which is referred as suspension history. The third load history representing a vibration with nearly zero mean loads, which is referred as the bracket history (Tucker and Bussa, 1975; Rahman *et al*., 2007). These histories were scaled to two peak strain levels and used as full-length histories. The variable amplitude load-time histories are shown in Fig. 4. The terms of SAETRN, SAESUS and SAEBKT represent the load-time history for the transmission, suspension and bracket, respectively. The considered load-time histories are based on the SAE's profile. In addition, I-N, ASTM composite mission typical fighter loading history and ASTM composite mission typical transport loading history, respectively (Tucker and Bussa, 1975; Rahman *et al*., 2007). The abscissa is the time in seconds.

RESULTS AND DISCUSSION

Finite element modeling: There are a number of safety-critical component of the free piston engine. The cylinder head is the one of the important and safety-critical components of the free piston engine. There are several contact areas including the cylinder block, gasket and hole for bolt. Therefore, constraints are employed for the following purposes: (i) to specify the prescribed enforce displacements, (ii) to simulate the continuous behavior of displacement in the interface area and (iii) to enforce rest condition in the specified directions at grid points of reaction. Three-dimensional model of the free piston linear engine cylinder head was developed using CATIA® software. A 10 nodes tetrahedral element was used for the solid mesh. Sensitivity analysis was performed to obtain the optimum element size. These analyses were performed iteratively at different element lengths until the solution

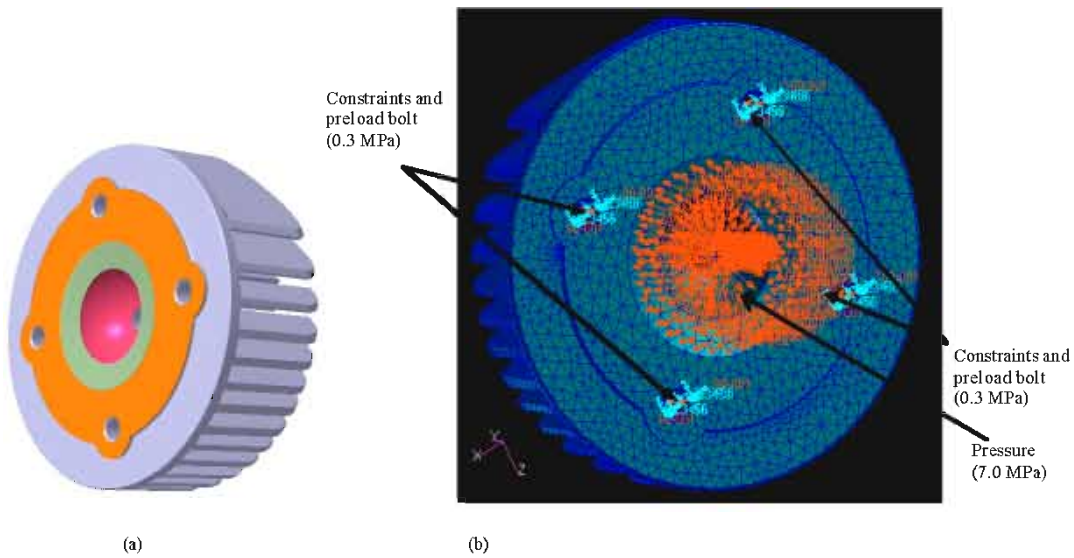

Fig. 5: (a) Structural model and (b) three-dimensional FE model, loading and constraints

obtained appropriate accuracy. Convergence of the stresses was observed, as the mesh size was successively refined. The element size of 1.25 mm was finally considered. A pressure of 7.0 MPa was applied on the surface of the cylinder head chamber generating a compressive load. A pressure of 0.3 MPa was applied on the bolt-hole surface generating a preload. This preload is obtained according to the RB and W recommendations (Shigley *et al*., 2004). In addition, 0.3 MPa pressure was applied on the gasket surface. Three-dimensional FEM model, loading and constraints on the cylinder head is shown in Fig. 5.

Selection of the mesh type: Mesh study is performed on the FE model to ensure sufficiently fine sizes are employed for accuracy of calculated results but at competitive cost (CPU time). In the process, specific field variable is selected and its convergence is monitored and evaluated. Selecting the right techniques of meshing are based on the geometry, model topology, analysis objectives and engineering judgment. Triparametric solids with the topological shape of a brick or wedge can be meshed either hexahedral or wedge elements. Any other form of the triparametric solid can only be meshed with tetrahedral elements. Solid that have more than six faces must first be modified and decomposed before meshing. The auto tetrahedral meshing approach is a highly automated technique for meshing solid regions of the geometry. It crates a mesh of tetrahedral elements for any closed solid including boundary representation solid. Tetrahedral meshing produces high quality meshing for boundary representation solids model imported from the most CAD systems. Since the tetrahedral is found to be the best meshing technique, the 4 nodes tetrahedral (TET4) element version of the cylinder head was then used for the initial analysis. In addition, the TET4 compared to the 10 nodes tetrahedral (TET10) element mesh using the same global mesh length for the highest loading conditions (7.0 MPa) in the combustion chamber. The result shows that the TET10 mesh predicted higher von Mises stresses than that the TET4 mesh (Fig. 6).

Figure 7 shows the von Mises stresses contour for TET4 and TET10 meshes element at a high load level. As shown in Fig. 7, there is quite a difference between the two, but the TET4 mesh is still capable of identifying critical areas. The TET10 mesh is presumed to represent a more accurate solution since TET4 meshes are known to be dreadfully stiff (Felippa, 2008). TET4 employed a linear order interpolation function while TET10 used quadratic order interpolation function. For the same element size, the TET10 is expected to be able to capture the high stress concentration associated with the bolt holes. Both of the meshes have some distorted elements cause error to the modeling in areas of elevated stress. In the mesh study of FE analysis, these areas should be remeshed and further refined to check for solution convergence. In addition, the modeling of joints using MPC elements may also introduce errors to the overall results.

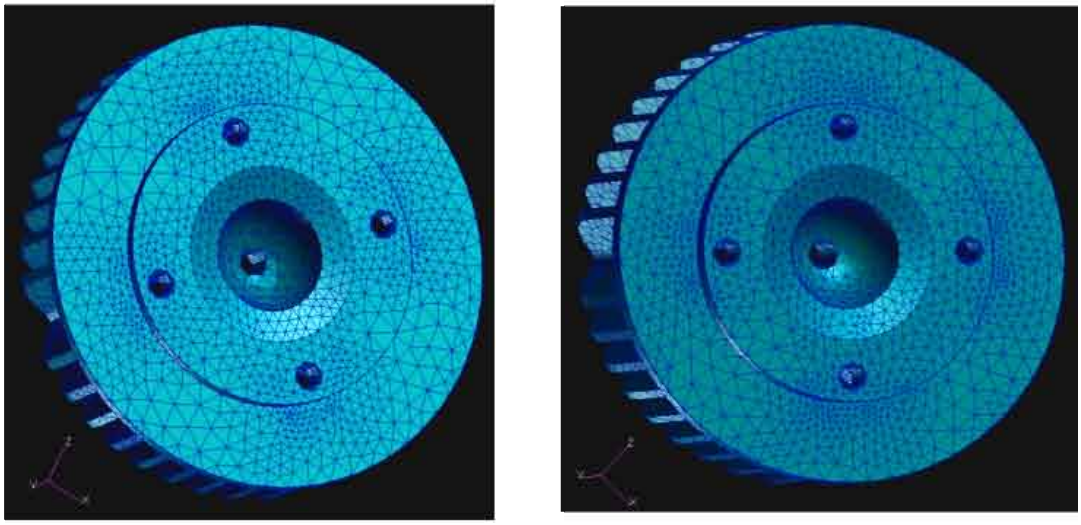

(a) TET4, 83259 elements (b) TET10, 83353 elements

Fig. 6: Finite element meshing for (a) TET4 and (b) TET10 using the same global mesh length

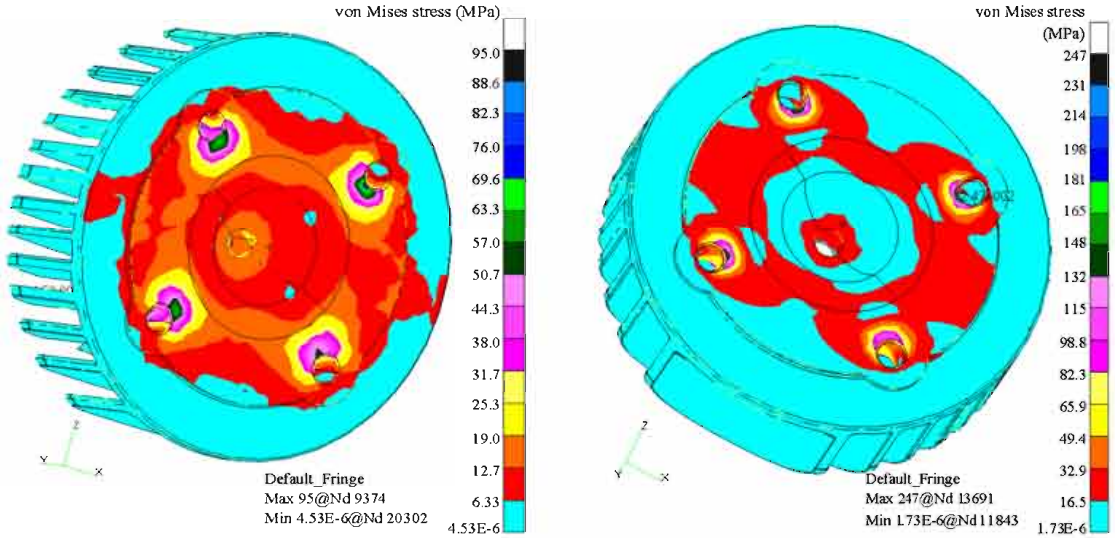

(a) (b)

Fig. 7: von Mises stresses contours (a) TET4 and (b) TET10 meshes at a high load level

The preliminary analysis using the TET4 mesh showed that the areas of stress were confined to a single region. Further analysis is confined to the region with the highest tensile and compressive stresses using the TET10 mesh. The TET4 simulation is compared to the same simulation using the TET10 mesh. Figure 7 shows that the TET10 mesh predicts higher von Mises stresses than the TET4 mesh. Specifically, the TET10 mesh predicts the maximum von Mises stress of 247 MPa. Figure 8 shows the fatigue life computed using the Coffin-Manson criteria for TET4 and TET10 meshes. It is observed from Fig. 8 that the TET10 mesh yields a much more conservative prediction of approximately $10^{6.832}$ or 6.79×10^{6} sec as opposed to $10^{8.25}$ or 1.78×10^{8} sec for the TET4 mesh. Units

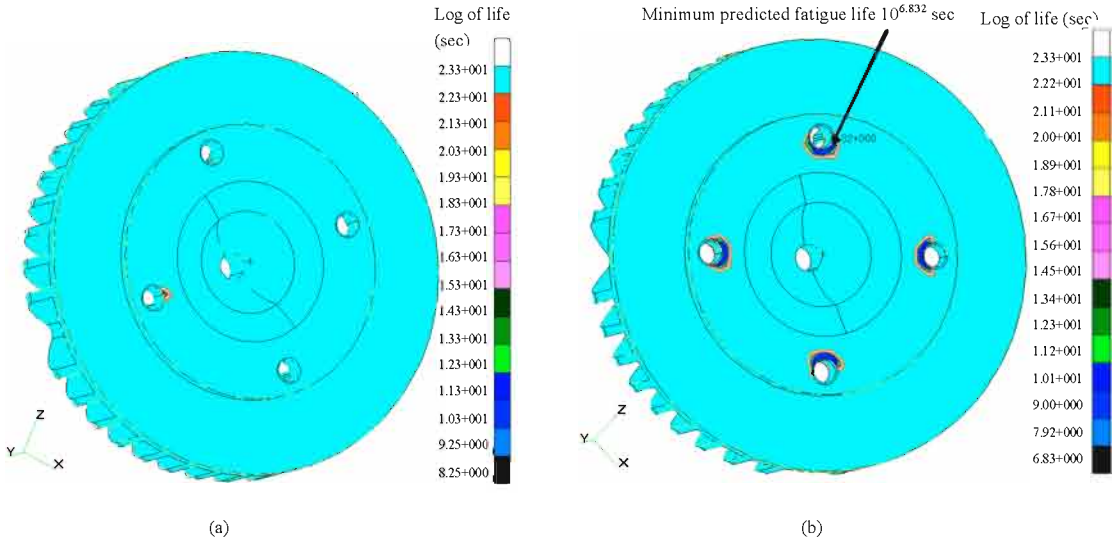

Fig. 8: Predicted fatigue life contours plotted for TET4 and TET10 meshes using the Coffin-Manson method

are in logarithm of seconds to failure, where 1 sec refers to the 50 cycles simulation.

Identification of the mesh convergence: The convergence of the stress was considered as the main criteria to select the mesh size. Detailed refinement at the critical points would result in extremely lengthy analysis time and was, therefore, avoided. The finite element mesh was generated using the tetrahedral elements with various element lengths of 5 mm (25936 elements), 4.5 mm (30650 elements), 4 mm (45746 elements), 3.5 mm (57462 elements), 3 mm (79413 element), 2.5 mm (111577 elements), 2 mm (152133 elements), 1.75 mm (201160 elements), 1.5 mm (286832 elements), 1.25 mm (289142 elements) and 1 mm (353412 elements). The maximum principal stresses were checked for convergence at the critical locations, as shown in Fig. 9. It is observed that the convergence has been obtained for the global mesh size of 1.0 mm due to it tends to the actual stress value. The maximum percentage difference between the stress values observed between the two models (the one with 289142 elements and other one with 353412 elements) is 0.73%, which is small. Thus, the mesh size 1.25 mm with 289142 elements was used for the FE analysis due to the limitation of the computational time and the storage capacity. Figure 9 shows the variation of the stress at the critical points of components. The global mesh size of 1.25 mm and local mesh size of 0.2 mm for the forged steel, cast aluminum and cast iron cylinder head were specified. Due to the higher stress concentration at the fillet of the cylinder head, large stress gradient existed at this location and therefore, more refined mesh size was implemented.

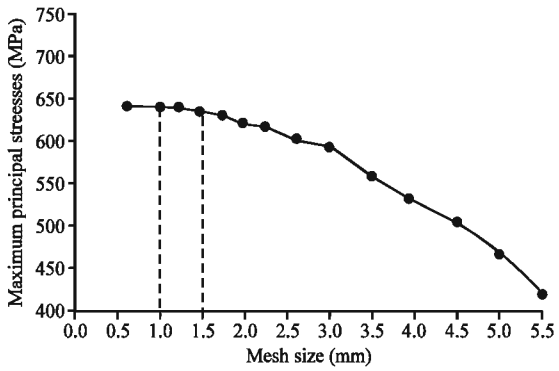

Fig. 9: Maximum principal stresses versus mesh size at critical location of cylinder head to check mesh convergence

Linear static stress analysis: The linear static analysis was performed using Msc. NASTRAN® finite element software to determine the stress and strain results from the finite element model. The material models utilized in this work consist of a linear elastic, isotropic material. Summary of the mechanical properties of forged, cast aluminum and cast iron are listed in Table 1. The choice of the linear elastic material model is essentially mandated. Model loading consists of the applied mechanical load, which is modeled as the load control and the displacement control. The bolt-holes areas were found to experience the highest stresses. The results of the maximum principal stresses and strains are used for the subsequent fatigue life analysis and comparisons. The maximum principal stresses distributions of the cylinder head for the linear

Table 1: Summary of the monotonic and cyclic properties of forged, cast aluminum and cast iron

	Material model		
Mechanical properties	Forged steel 11V37	Cast aluminum A356-T6	Cast iron 65-45-12
Monotonic properties			
Modulus of elasticity (E, GPa)	201.500	78.100	193.000
Yield strength (0.2% offset) (S_y, MPa)	556.200	232. 40	300.000
Ultimate tensile strength (S_u, MPa)	821.200	302.700	471.200
Percent elongation (EL, %)	21.000	5.000	10.000
Percent reduction in area (RA, %)	37.000	10.000	25.000
Strength coefficient (K, MPa)	1347.300	417.800	796.500
Strain hardening exponent (n)	0.157	0.096	0.187
True fracture strength (σ_f, MPa)	496.000	301.000	219.200
True fracture ductility (ε_f %)	47.000	10.000	28.000
Cyclic properties			
Cyclic modulus of elasticity (E′, GPa)	196.900	73.300	169.400
Fatigue strength coefficient (σ'_f, MPa)	1156.800	665.900	760.800
Fatigue strength exponent (b)	-0.082	-0.117	-0.076
Fatigue ductility coefficient (ε'_f)	3.032	0.094	0.864
Fatigue ductility exponent (c)	-0.791	-0.610	-0.771
Fatigue strength (S_f @ 10^6 cycles, MPa)	352.000	122.000	253.000
Cyclic yield strength (S'_y, MPa)	541.200	290.700	407.300
Cyclic strength coefficient (K′, MPa)	1269.500	430.300	649.100
Cyclic strain hardening exponent (n′)	0.137	0.063	0.075

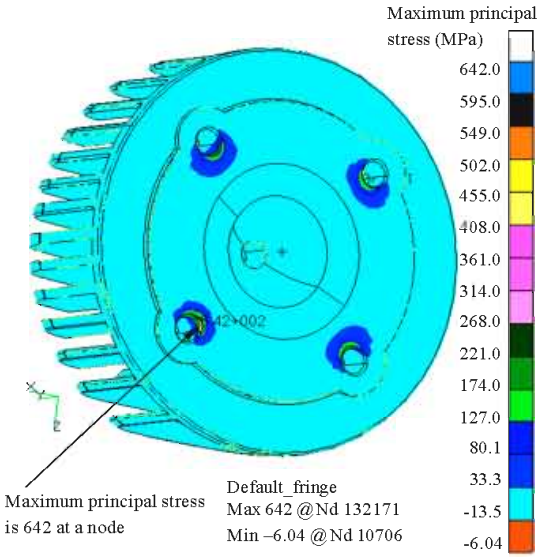

Fig. 10: Maximum principal stresses contour plotted for the cast aluminum A356-T6 with SAETRN loading

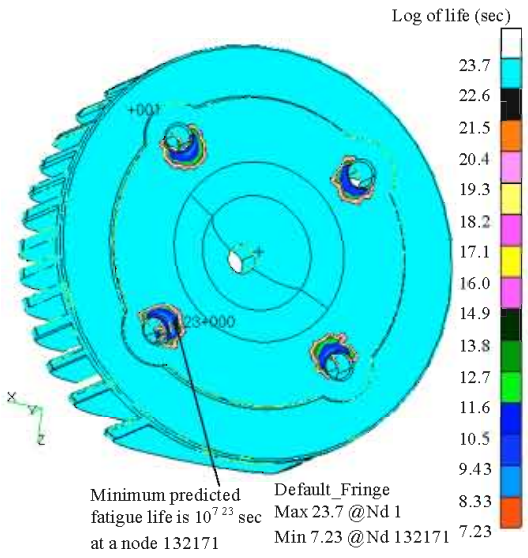

Fig. 11: Predicted life contours plotted in terms of log of life for the SAETRN loading conditions for A356T6 using

static analysis is presented in Fig. 10 for cast aluminum with SAETRN loading. From the acquired results, the maximum principal stresses of 642 MPa occurring at node 132171 was obtained for cast aluminum.

Fatigue analysis: The fatigue life of the cylinder head is predicted for material A356-T6 and SAETRN loading condition material acting on the cylinder head of the linear generator engine using the stress-life approach. The materials S-N curves are considered in this analysis. The fatigue equivalent unit is 3000 cpm (cycle per min) of the time history. The result of the predicted fatigue life of the cylinder head corresponding to 99.8% reliability value is shown in Fig. 11 for cast aluminum. The critical location is also shown in Fig. 11 at node132171. The predicted minimum and maximum fatigue life are $10^{7.23}$ and $10^{23.7}$ sec respectively. The rainflow cycle counting method was employed in this analysis to counts the number of cycles

Table 2: Predicted fatigue life at critical location with mean stress effect

	Material AA 6061-T6			Material A356-T6		
Loading conditions	No mean stress (R=-1)	Goodman	Gerber	No mean stress (R=-1)	Goodman	Gerber
SAETRN	4.80×10^{6}	4.24×10^{5}	3.43×10^{6}	1.70×10^{7}	3.58×10^{6}	1.21×10^{7}
SAESUS	6.07×10^{8}	8.51×10^{9}	1.15×10^{9}	2.19×10^{9}	1.96×10^{10}	3.29×10^{9}
SAEBKT	6.29×10^{6}	6.38×10^{6}	6.08×10^{6}	2.13×10^{8}	2.24×10^{8}	2.01×10^{8}
I-N	6.70×10^{8}	3.45×10^{6}	1.27×10^{8}	2.63×10^{10}	4.76×10^{8}	8.89×10^{9}
R-C	1.04×10^{8}	1.11×10^{6}	2.77×10^{7}	4.26×10^{9}	1.23×10^{8}	1.63×10^{9}
TRANSP	1.66×10^{8}	3.28×10^{6}	6.72×10^{7}	8.92×10^{9}	3.16×10^{8}	4.00×10^{9}

and determines their range and mean. The fatigue life is expressed in seconds of the variable amplitude loading conditions. It is observed that the bolt-hole edges of the cylinder head is the most critical positions among the component.

The minimum predicted fatigue life at critical location (node 132171) for the various loading histories and materials using the stress-life method are tabulated in Table 2. Two mean stress correction methods namely Goodman model and Gerber model are considered in this study. Examining the data in Table 2, the Goodman mean stress correction method gives the most conservative prediction when the time histories are predominantly tensile mean. All the three methods give the approximately similar results when using the time histories are roughly zero mean loadings, however, the Gerber mean stress correction gives conservative prediction. In addition no mean stress (R = -1) method found to be the conservative prediction when the time histories are predominantly compressive mean.

Effect of material and component S-N curves: There are two type of stress-life (S-N) curves. The first is the nominal or component S-N curve where the stress plotted on the Y-axis is not the actual stress where failure occurs i.e., there is a built-in geometric stress concentration factor, K_t. The use of this type of S-N curve is only valid when the stress in a nominal or reference area is used to compute life. This approach takes no account of localized plasticity effects such as might be found at a stress raiser. The effects of such discontinuities must be taken into account through the S-N damage curve itself. The second type of S-N curve is the local stress or material S-N curve. This curve has associated with it a K_t value of 1.0, i.e., the stress on the Y-axis is a local stress which causes fatigue. No reference area is needed as the results at each node or element may be used directly. Materials S-N are S-N curves generated from the elastic part of the strain controlled fatigue tests or S-N curves for which $K_t = 1.0$ and component S-N are generated directly from the stress based fatigue tests on components and the associated

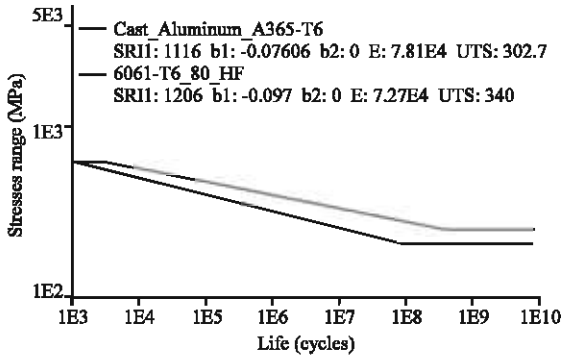

Fig. 12: Stress amplitude versus reversals to failure for A356-T6 and AA6061-T6-80-CF materials

$K_t>1.0$. The material S-N curves are the component S-N curves except it has been scaled by the K_t value, where K_t is the geometry compensation factor or the theoretical elastic stress concentration factor. The material S-N curve relates elastic stress (S) to the number of cycles (N) required causing failure. This S-N curve represents the relationship between nominal stresses at the point of failure in a material to life. Such curves can be used for detecting failure locations and estimating life across an entire finite element model for which appropriate elastic stresses have been calculated. Component (global) S-N curve can be used to estimate how long the component as a whole will lasting under cyclic loading with the failure location being defined by the component itself during the cyclic testing process. The component S-N approach is very useful in situations where an accurate description of local stress, either elastic or elastic-plastic, is difficult to achieve. Figure 12 presents the S-N behaviour of the A356-T6 and AA6061-T6-80-CF materials. This S-N curve is called material S-N curve that represents the material and it is independent of the geometry. The S-N fatigue analysis method is generally only good for the high cycle fatigue problems, which means that the number of the cycles to failure is extremely high.

Table 3 listed the comparison between the material S-N and component S-N approaches for the SAETRN

Table 3: Comparisons between the material and component S-N Approaches for SAETRN loading conditions

	Material S-N approach			Component S-N approach		
Materials	No mean stress (R=-1)	Goodman	Gerber	No mean stress (R=-1)	Goodman	Gerber
6053-T6	2.42×10^{5}	1.31×10^{5}	2.24×10^{5}	2.18×10^{6}	4.57×10^{6}	2.96×10^{6}
6061-T6	4.80×10^{6}	4.24×10^{5}	3.43×10^{6}	3.71×10^{7}	2.15×10^{7}	8.48×10^{6}
6061-T91	2.13×10^{8}	4.14×10^{7}	1.81×10^{8}	8.00×10^{8}	4.84×10^{8}	2.82×10^{8}
6066-T6	1.43×10^{8}	6.84×10^{7}	1.22×10^{8}	5.16×10^{8}	3.51×10^{8}	1.79×10^{8}
6070-T6	8.86×10^{7}	3.81×10^{7}	7.60×10^{7}	6.46×10^{8}	2.40×10^{8}	1.22×10^{8}
6151-T6	1.43×10^{7}	8.26×10^{6}	1.26×10^{7}	9.32×10^{7}	7.88×10^{7}	3.85×10^{7}
6262-T8	6.29×10^{6}	2.51×10^{6}	5.61×10^{6}	5.71×10^{7}	3.15×10^{7}	1.48×10^{7}
6262-T9	1.80×10^{8}	9.54×10^{7}	1.54×10^{8}	7.64×10^{8}	4.24×10^{8}	2.18×10^{8}
6951-T6	3.81×10^{5}	1.88×10^{5}	4.82×10^{5}	3.59×10^{6}	8.01×10^{6}	3.94×10^{6}

Table 4: Predicted fatigue life at critical location (node 49360) for various materials and loading conditions

	Predicted fatigue life in seconds for Goodman mean correction method					
Materials	SAETRN	SAESUS	SAEBRAKT	I-N	R-C	TRANSP
6053-T6	2.96×10^{6}	1.21×10^{9}	4.57×10^{6}	3.58×10^{5}	1.28×10^{5}	8.92×10^{4}
6061-T6	8.48×10^{6}	7.29×10^{9}	3.15×10^{7}	8.74×10^{6}	2.65×10^{6}	3.28×10^{6}
6061-T91	2.82×10^{8}	9.99×10^{10}	4.84×10^{8}	4.69×10^{8}	1.21×10^{8}	3.16×10^{8}
6066-T6	1.79×10^{8}	7.63×10^{10}	3.51×10^{8}	2.98×10^{8}	7.96×10^{7}	1.91×10^{8}
6070-T6	1.22×10^{8}	5.51×10^{10}	2.40×10^{8}	1.79×10^{8}	4.79×10^{7}	1.04×10^{8}
6151-T6	3.85×10^{7}	1.35×10^{8}	6.88×10^{6}	2.28×10^{7}	6.62×10^{6}	9.84×10^{6}
6262-T8	1.48×10^{7}	7.29×10^{9}	3.15×10^{7}	8.74×10^{6}	2.65×10^{6}	3.28×10^{6}
6262-T9	2.18×10^{8}	8.94×10^{10}	4.24×10^{8}	3.84×10^{8}	1.02×10^{8}	2.58×10^{8}
6951-T6	3.94×10^{6}	1.98×10^{9}	8.01×10^{6}	9.46×10^{5}	2.17×10^{5}	6.96×10^{5}

loading conditions. It is observed that the Gerber mean stress correction method is most conservative prediction for the component S-N curve approach for all materials and the material S-N approach. In addition, the materials AA6053-T6 and AA6951-T6 gives the most conservative results with zero mean stress. It is also observed that the component S-N approach gives the higher life than the material S-N approach.

Table 4 listed the minimum predicted life for various materials and loading conditions for the Gerber mean stress correction method using the component S-N curves. It can be seen that AA6061-T91 is consistently has higher life than other materials for all loading conditions.

Effect of certainty of survival: From Fig. 13, it can be seen that the fatigue life decreases gradually as the design criterion increases to 99.9% (certainty of survival 99.9%). This is due to the effect of the probabilistic nature of the fatigue and the scatter associated with the S-N curves themselves. The material parameters associated with the S-N curves have considered the effect with the standard error of Log (N) determined by the regression analysis of the raw data. It is recommend that 99.9% (99.9% certainty of survival) to be found as the design criterion. The larger the scatter in the original S-N data that generates the curve, the less certain will be of survival. For both cases,

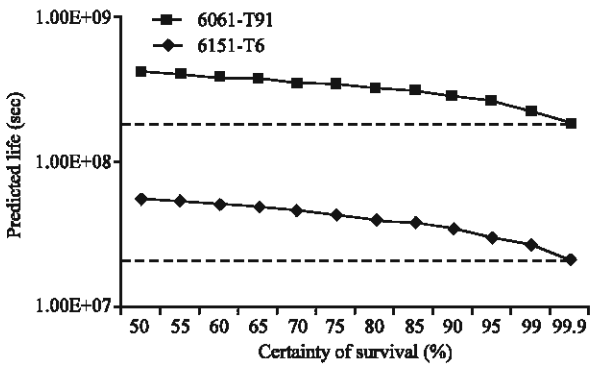

Fig. 13: The effect of certainty of survival on the fatigue life

it can be seen that 99.9% certainty of survival gives more conservative results. Figure 13 also shows that the AA6061-T91 has higher predicted fatigue life based on the S-N curves. This is due to the effect of the probabilistic nature of S-N curves where the scatter in the S-N data for AA6061-T91 is larger than for AA6151-T6. The results of the fatigue life contours for the SAETRN loading conditions with 99.9 and 50% certainty of survival are shown in Fig. 14. It is clearly shows that the 99.9% certainty of survival is more damage than 50% certainty of survival cases due to the effect of the probabilistic nature of fatigue and the scatter associated with the S-N curves.

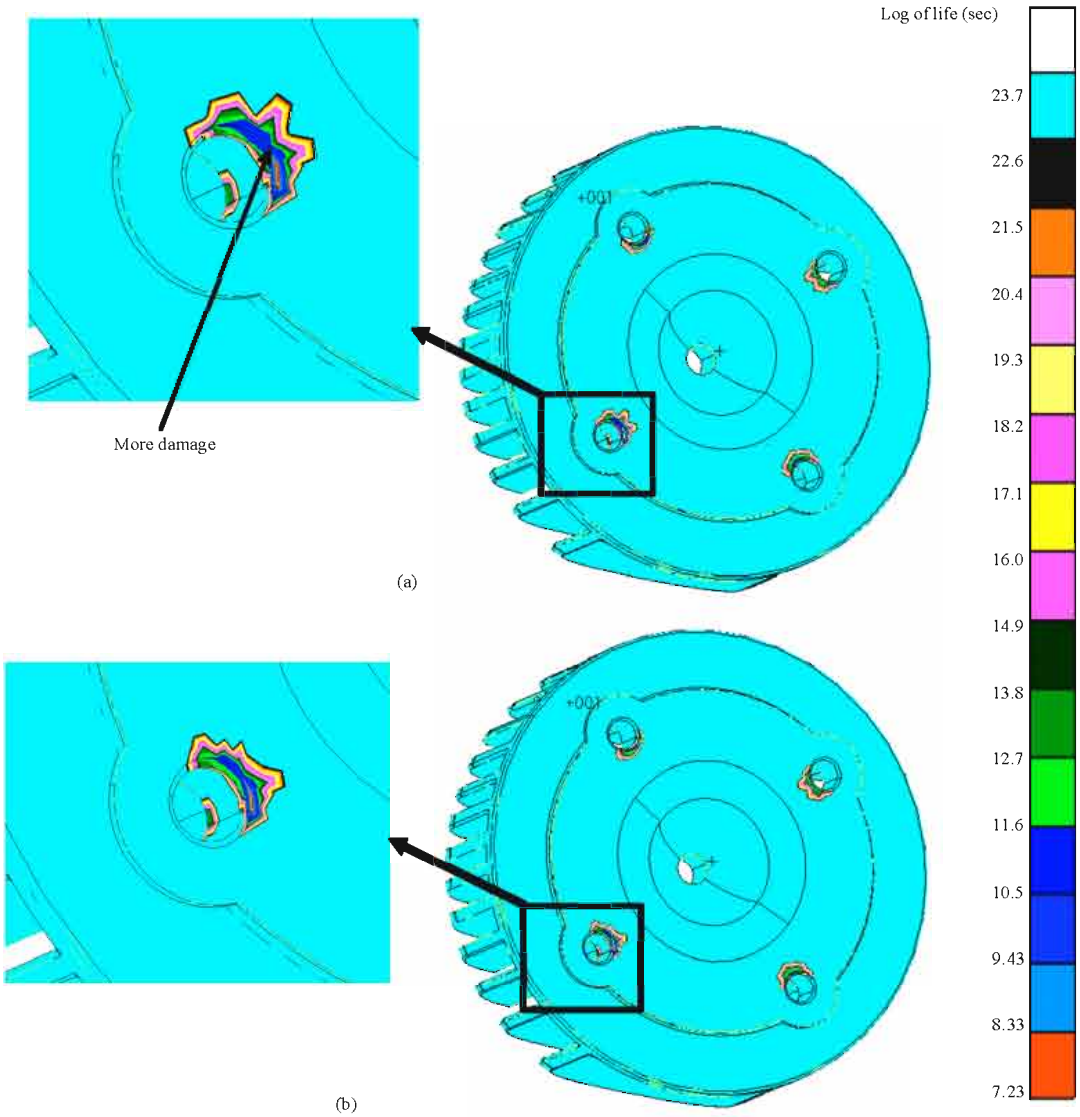

Fig. 14: Fatigue life contours plotted of the cylinder head for the SAETRN loading conditions with (a) certainty of survival 99.9% and (b) certainty of survival 50%

CONCLUSION

A computational approach of the fatigue analysis methodology for the life prediction is presented. Based on the conducted study, several conclusions can be drawn with regard to the fatigue life prediction. (i) No locations with serious failure potential were predicted for a target life, (ii) No design modifications were deemed necessary for the first prototype, (iii) The influences of mean stress correction are different for the compressive and the tensile mean stress. It is concluded that the compressive mean stresses are found to be beneficial and the tensile mean stresses are detrimental to the fatigue life, (iv) It is observed that the Goodman mean stress correction method for the stress-life approach gives the most conservative results when the time histories are predominantly tensile mean and (v) From the results, the effect of certainty of survival are significantly influence on the fatigue life and 99.9% certainty of survival gives the most conservative prediction due to the probabilistic nature of fatigue and the scatter associated with the S-N curves themselves and recommended as the design criteria.

ACKNOWLEDGMENTS

The authors would like to thank Department of Mechanical and Materials Engineering, University Kebangsaan Malaysia for provided lab facilities. The authors are grateful to the Universiti Malaysia Pahang for provided the financial support.

REFERENCES

Achten, P.A.J., 1994. A review of free piston engine concepts. SAE Technical Paper No. 941776. http://www.sae.org/technical/papers/941776.

Arshad, W.M., P. Thelin, T. Bäckström and C. Sadarangani, 2004. Use of transverse flux machines in a free piston generator. IEEE Trans. Ind. Appl., 40: 1092-1100.

Fatigure, M., 2005. User manual. Los Angles: MSc. Software Corporation. http://mscsoftware.com/.

Felippa, C.A., 2008. Advanced finite element methods. http://caswww.colorado.edu/courses.d/AFM.d/Home.html.

Lee, Y.L. and D. Taylor, 2005. Stress based fatigue analysis and design. Fatigue Testing and Analysis: Theory and Practice. Elsevier, pp: 103-180.

Lee, Y.L., J. Pan, R.B. Hathaway and M.E. Barkey, 2005. Fatigue Testing and Analysis: Theory and Practice. 1st Edn., Butterworth Heinrahmanemann, New York, ISBN: 978-0-7506-7719-6.

Mikalsen, R. and A.P. Roskilly, 2007. A review of free piston engine history and applications. Applied Therm. Eng., 27: 2339-2352.

Mikalsen, R. and A.P. Roskilly, 2008a. The design and simulation of a two-stroke free piston compression ignition engine for electrical power generation. Applied Therm. Eng., 28: 589-600.

Mikalsen, R. and A.P. Roskilly, 2008b. Performance simulation of a spark ignited free piston engine generator. Applied Therm. Eng., 28: 1726-1733.

Rahman, M.M. A.K. Ariffin, N. Jamaludin and C.H.C. Haron, 2006. Durability assessment of a new free piston spark ignition linear engine: A computational approach. J. Tech. A, 45: 81-102.

Rahman, M.M., A.K. Ariffin, S. Abdullah and N. Jamaludin, 2007. Finite element based durability assessment of a free piston linear engine component. SDHM, 3: 1-14.

Shigley, J.E., C.R. Mischke and R.G. Budynas, 2004. Mechanical Engineering Design. 7th Edn., McGraw Hill, New York, ISBN 978-0072520361.

Somhorst, J.H.E. and P.A.J. Achten, 1996. The combustion process in a di-diesel hydraulic free piston engine. SAE Technical Paper No 960032. http://www.sae.org/technical/papers/960032.

Tucker, L. and S. Bussa, 1975. The SAE cumulative fatigue damage test program. SAE Technical Paper No. 750038. http://www.sae.org/technical/papers/750038.

Zoroufi, M. and A. Fatemi, 2004. Fatigue life comparisons of competing manufacturing processes: A study of steering knuckle. SAE Transactions, SAE Technical Paper No. 2004-01-0628. http://www.sae.org/technical/papers/2004-01-0628.